

Intermediate-boson and dilepton production in hadronic interactions*

R. B. Palmer, E. A. Paschos, N. P. Samios, and Ling-Lie Wang

Brookhaven National Laboratory, Upton, New York 11973

(Received 10 November 1975)

Various relations are obtained between dilepton and intermediate-boson (W) production cross sections. It is pointed out that if the dilepton production obeys a scaling law, then its measurement at presently available energies can provide a lower bound for the production of W bosons in future high-energy experiments. We also calculate W production using a Drell-Yan model with and without color. We find that the model without color is quite successful when compared with the dilepton production data. Estimates of the leptonic and hadronic decay rates of the W boson are also given.

I. INTRODUCTION

The most direct test of the underlying theory of weak interactions is the search for intermediate vector bosons.¹ In addition to the long-standing prediction of charged mediators of the weak force (W^\pm particles), gauge theories require the existence of neutral counterparts (W^0 particles) which mediate neutral currents. The observation of neutral currents in numerous neutrino experiments provides strong support² for the existence of a triplet of intermediate vector bosons.

The most promising way of producing them is with proton-proton colliding beams,³ where they can be identified by their leptonic decays. In any unified theory of weak and electromagnetic interactions the expected masses are of order $(\alpha/G)^{1/2}$, or roughly 30–100 GeV/ c^2 . Such masses are within the reach of the next generation of colliding ring facilities. For this reason we consider it timely to summarize the theoretical expectations for their production.

Our approach to the problem is at two levels. In the first we derive rigorous bounds⁴ for the production of W 's in terms of electromagnetic production of dileptons in the $p\bar{p}$ reaction,

$$p + \bar{p} \rightarrow l + \bar{l} + X \quad (1.1)$$

where l denotes a lepton and \bar{l} denotes its anti-particle. For charged mesons the relations follow from the conserved-vector-current hypothesis. For neutral mesons the bounds depend, in addition, on the particular gauge theory under consideration. The practical value of the bounds rests on the fact that we can relate the production of W^\pm or W^0 to the electromagnetic production of $l\bar{l}$ continuum at the same mass and at the same center-of-mass energy. In the absence of measurements for reaction (1.1) at very high energies, we investigate data at presently available energies searching for the scaling limit of the reaction. A summary of existing results indicates

that the data fall on smooth curve, suggesting that the dimensionless cross section $M^3 d\sigma/dM$ for dilepton production is a function of s/M^2 , where M is the dilepton mass. If this is indeed the case, we can in turn calculate the lower bounds for the production of W bosons.

In the second approach, we make use of a Drell-Yan model.^{5,6} All previous results can be reproduced in the model, since the general principles involved in deriving the bounds are naturally incorporated within the model. We choose the quark distributions from the existing fits⁶ to electron and neutrino inelastic scattering, which give, in addition, the best agreement for the electromagnetic production of $l\bar{l}$ in $p\bar{p}$ collisions. We then calculate the W^\pm production in both $p\bar{p}$ and $p\bar{p}$ reactions. The model predicts that in $p\bar{p}$ reactions the production of W^+ is larger than the production of W^- owing to the fact that there are more positive quarks in protons. Model calculations and detailed curves are included in Sec. III. Section IV summarizes the expectations for the W decay widths.

II. GENERAL BOUNDS

In all the processes under consideration, we assume that the dileptons couple directly to a weak or electromagnetic current, which in turn couples to the hadronic system. The lepton vertex is well determined by the theory of electromagnetic and weak interactions, and the main interest is in the couplings of the currents to the hadrons as shown in Fig. 1(a). The conserved-vector-current hypothesis tells us that the cross sections for the production of W 's with different charges are related to each other and also to the electromagnetic matrix elements.

We define the cross sections

$$\sigma_p^{i,\nu} = \sigma(pp \rightarrow v^i + X), \quad (2.1)$$

$$\sigma_n^{i,\nu} = \sigma(pn \rightarrow v^i + X), \quad (2.2)$$

$$\sigma_p^{i,a} = \sigma(pp \rightarrow a^i + X), \quad (2.3)$$

$$\sigma_n^{i,a} = \sigma(pn \rightarrow a^i + X), \quad (2.4)$$

where v^i (a^i) denotes the vector (axial-vector) current produced and the superscript i indicates its charged state. Here we only consider isovector currents. To make an isospin analysis we define $V_j^{(k)}, A_j^{(k)}$ as the contributions of the isovector part of the vector and axial-vector currents to the above cross sections, where $k = (0, 1, 2)$ is the isospin of X and $j = 1, 0$ distinguishes the amplitudes originating from an initial state of total isospin 1 or 0. For cross sections involving mixed isospin in the initial states, we use $V_{jj'}^{(k)}, A_{jj'}^{(k)}$. See Fig. 1(a).

The isospin analysis gives

$$\sigma_p^{-,\nu} = 2V_1^{(2)}, \quad (2.5)$$

$$\sigma_p^{+,\nu} = \frac{1}{3}V_1^{(2)} + V_1^{(1)} + \frac{2}{3}V_1^{(0)}, \quad (2.6)$$

$$\sigma_p^{3,\nu} = \frac{1}{2}V_1^{(2)} + \frac{1}{2}V_1^{(1)}, \quad (2.7)$$

$$\sigma_n^{-,\nu} = \frac{1}{2}V_1^{(2)} + \frac{1}{2}V_1^{(1)} + V_{1,0}^{(1)} + V_0^{(1)}, \quad (2.8)$$

$$\sigma_n^{+,\nu} = \frac{1}{2}V_1^{(2)} + \frac{1}{2}V_1^{(1)} - V_{1,0}^{(1)} + V_0^{(1)}, \quad (2.9)$$

$$\sigma_n^{3,\nu} = \frac{1}{3}V_1^{(2)} + \frac{1}{6}V_1^{(0)} + \frac{1}{2}V_0^{(1)}. \quad (2.10)$$

One can read off directly several inequalities relevant to pp collisions. For example

$$\sigma_p^{-,\nu} + \sigma_p^{+,\nu} \geq \frac{1}{3}\sigma_p^{-,\nu} + \sigma_p^{+,\nu} \geq 2\sigma_p^{3,\nu}. \quad (2.11)$$

This means that in pp collisions the sum of W^+ and W^- production is greater than twice the W^0 production. We also have

$$\sigma_p^{+,\nu} \geq \frac{2}{3}\sigma_p^{3,\nu}, \quad (2.12)$$

$$\sigma_n^{3,\nu} \geq \frac{1}{6}\sigma_p^{-,\nu}. \quad (2.13)$$

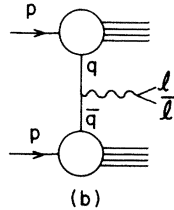
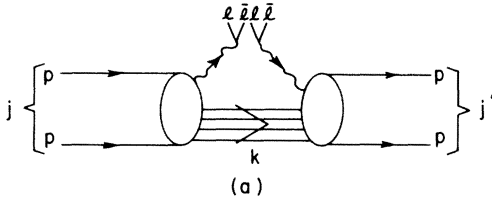


FIG. 1. (a) Lepton-pair production in pp reaction. (b) Electromagnetic production of lepton pair in the Drell-Yan model.

Alternatively defining cross sections on isoscalar targets by

$$\sigma_N^{+,\nu} + \sigma_N^{-,\nu} = \frac{1}{4}(\sigma_p^{+,\nu} + \sigma_p^{-,\nu} + \sigma_n^{+,\nu} + \sigma_n^{-,\nu}), \quad (2.14)$$

$$\sigma_N^{3,\nu} = \frac{1}{2}(\sigma_p^{3,\nu} + \sigma_n^{3,\nu}), \quad (2.15)$$

we obtain a relation which already appears in the literature,⁴

$$\sigma_N^{+,\nu} + \sigma_N^{-,\nu} \geq 2\sigma_N^{3,\nu}. \quad (2.16)$$

There are other relations among cross sections on neutron targets which can easily be obtained from Eqs. (2.8)–(2.10). Similar relations can be obtained for axial-vector cross sections.

The discussion so far has neglected the vector-axial-vector interference terms because such terms do not occur in the total production rate (a pseudoscalar cannot be formed out of three four-vectors). Thus we can write the W -production cross section as the sum of two positive terms, one arising from the vector term alone and the other from the axial-vector term:

$$\sigma = \sigma^v + \sigma^a \geq \sigma^v. \quad (2.17)$$

Using the conserved-vector-current hypothesis, the production cross section $\sigma^{3,\nu}$ is related to the electromagnetic production (isovector part) of $l\bar{l}$ continuum, $d\sigma^{I=1}/dM$, by

$$\sigma^{3,\nu} = \frac{3GM^3}{8(2)^{1/2}\alpha^2} \frac{d\sigma^{I=1}}{dM}, \text{ at } M = m_W. \quad (2.18)$$

Equation (2.11) now becomes

$$\frac{1}{3}\sigma^- + \sigma^+ \geq \frac{3}{4} \frac{GM^3}{(2)^{1/2}\alpha^2} \frac{d\sigma}{dM} \approx 0.09M^3 \frac{d\sigma}{dM}, \text{ at } M = m_W, \quad (2.19)$$

or in differential form

$$\frac{1}{3} \frac{d\sigma^-}{d^3q} + \frac{d\sigma^+}{d^3q} \geq \frac{3GM^3}{4(2)^{1/2}\alpha^2} \frac{d\sigma}{d^3q dM}. \quad (2.20)$$

In the above inequality the axial-vector coupling of the W boson has been dropped together with the isoscalar part of the electromagnetic current. Both of the terms neglected can be determined within the parton model, where (2.19) is replaced by an equality to be discussed in the next section.

For the production of W^0 the results depend on the form of the weak neutral current. In Weinberg-Salam-type models⁷

$$\sigma^0 = (1 - 2\sin^2\theta_w)^2\sigma^{3,\nu} + \sigma^{3,a}, \quad (2.21)$$

which implies the inequality

$$\sigma^0 \geq \frac{3}{8} \frac{GM^3}{(2)^{1/2}\alpha^2} (1 - 2\sin^2\theta_w)^2 \frac{d\sigma^{I=1}}{dM}, \text{ at } M = m_W, \quad (2.22)$$

provided that isoscalar terms of the electromagnetic and the weak neutral current are neglected.

If we knew the electromagnetic cross section for the production of l^+l^- pairs then Eqs. (2.19) and (2.22) would provide lower bounds for the production of W 's. In the absence of such data at high energies it is noted that the dimensionless cross section $M^3 d\sigma/dM$ should scale as a function of s/M^2 for large s and M^2 . Thus one can look at the available data at lower energies in order to deduce the scaling law and then apply it at higher energies.

We use here three different experiments for $l\bar{l}$ continuum production:

(1) the old BNL-Columbia experiment⁸ at 29.5 GeV/c, with dilepton laboratory longitudinal-momentum cutoff at $p_l \geq 12.5$ GeV/c [the mass of $l\bar{l}$ varies from 1 GeV to 5 GeV (with the J and ψ' subtracted)],

(2) the MIT-BNL experiment⁹ at 30 GeV/c, with dilepton c.m. longitudinal momentum $p_l^* = 0$. [the dilepton mass is at 3 GeV (below the J peak)],

(3) the Fermilab-Columbia-Illinois experiment¹⁰ at 320 GeV/c with dilepton laboratory longitudinal-momentum cutoff at $p_l \geq 60$ GeV/c (the dilepton mass varies from 1 GeV to 2.8 GeV).

We see that these three experiments do not

overlap in the variable $Y_l \equiv p_l^*/\frac{1}{2}(s)^{1/2}$ and in the scaling variable M^2/s . Thus we have to rely on specific models to compare the data points. This will be discussed in the next section.

III. PARTON-MODEL CALCULATIONS

In this section we calculate W -meson production and lepton-pair-continuum production in the quark-parton model; see Fig. 1(b). In terms of the quark distributions of the proton, the $l\bar{l}$ -continuum-production cross section is given by

$$\frac{d\sigma^\pm}{dM} = \frac{G^2}{3\pi} \cos^2\theta_C M H^\pm(\tau), \quad (3.1)$$

where θ_C is the Cabibbo angle and M is the $l\bar{l}$ invariant mass.

$$H^\pm(\tau) \equiv \int_0^1 dx_1 \int_0^1 dx_2 \delta(x_1 x_2 - \tau) x_1 x_2 h^\pm(x_1, x_2),$$

$$\text{where } \tau \equiv M^2/s, \quad (3.2)$$

$$h^+(x_1, x_2) = u(x_1)\bar{d}(x_2) + u(x_2)\bar{d}(x_1),$$

$$h^-(x_1, x_2) = d(x_1)\bar{u}(x_2) + d(x_2)\bar{u}(x_1).$$

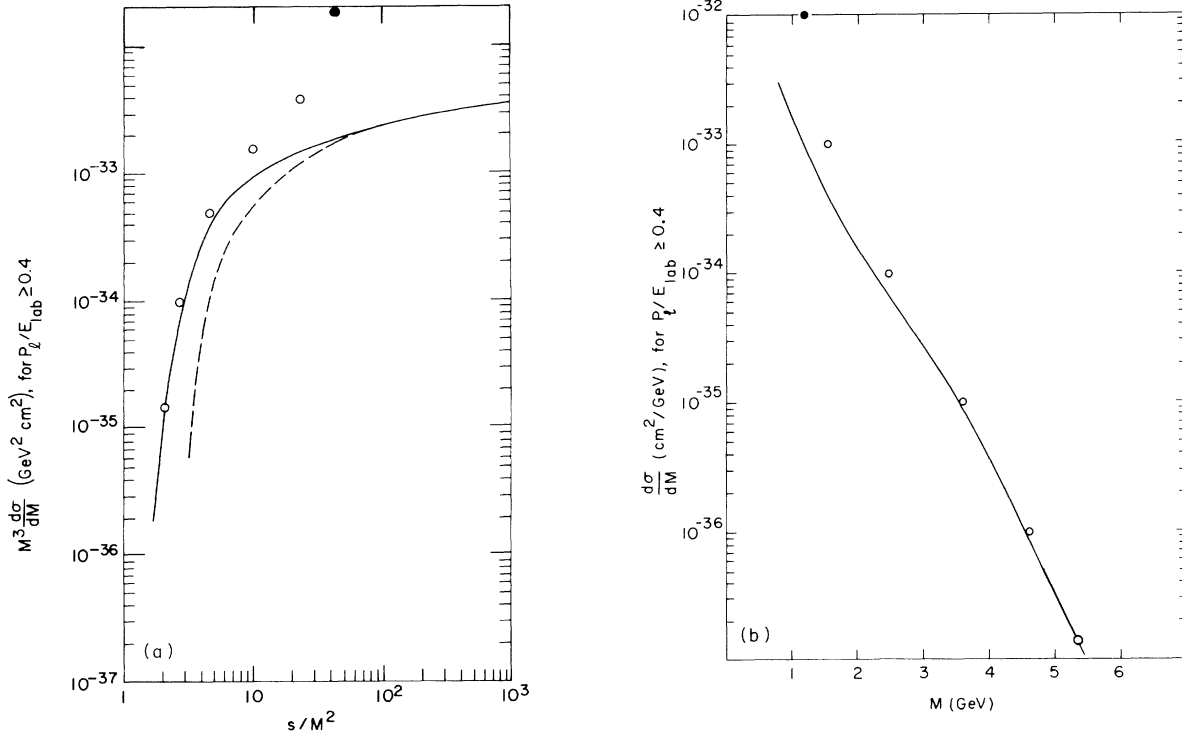


FIG. 2. (a) The plot of dimensionless cross section $M^3 d\sigma/dM$ as a function of s/M^2 , where M is the dilepton mass. The data points are from Ref. 8, $E_{\text{lab}} = 29.5$ GeV/c, $1 \text{ GeV} \leq M \leq 5 \text{ GeV}$, and dilepton laboratory $p_l > 12.5$ GeV/c. Data points for $M < 1.5$ GeV are made solid black. The solid curve is from the Drell-Yan-model calculations as discussed in Sec. III. The dotted curve is the same model calculation using the parametrization of Ref. 12. (b) The same calculation and data as in Fig. 3(a) replotted in $d\sigma/dM$ vs. M .

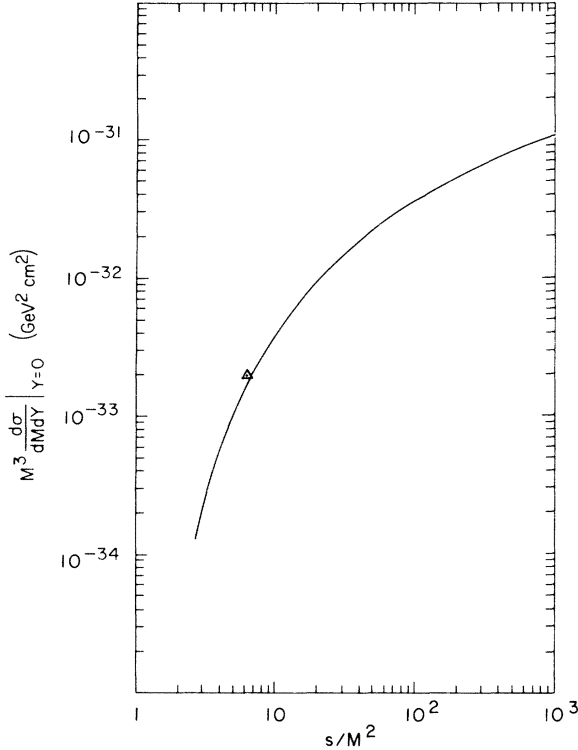


FIG. 3. $M^3 d\sigma/dM dY$ at $Y=0$ plotted as a function of s/M^2 , where $Y=P_1^*/\frac{1}{2}S^{1/2}$. The data point is from Ref. 9, $E_{\text{lab}} = 30 \text{ GeV}/c$, $M \approx 3 \text{ GeV}$ (below the J peak), center of mass $p_1^* \approx 0 \text{ GeV}/c$, and the solid curve is the model calculation discussed in Sec. III.

Here $u(x)$, $d(x)$, and $\bar{u}(x)$, $\bar{d}(x)$ are the quark and antiquark distributions in the proton if there is no color. The variable x_i is the fraction of the proton's momentum carried by the quark. (As usual the transverse momenta of the quarks have been taken to be 0.) For W^\pm production and its subsequent decay into leptons we have

$$\frac{d\sigma^\pm}{dM_{W \rightarrow l\nu}} = \frac{G^2}{12\pi} \frac{M^3}{(M - m_W)^2 + \Gamma^2/4} \cos^2\theta_C H^\pm(\tau), \quad (3.3)$$

where Γ is the full width of the W . The integrated cross section is

$$\sigma_W^\pm = (2)^{1/2} \pi G H^\pm(\tau) \cos^2\theta_C. \quad (3.4)$$

In order, however, to satisfy statistics and to obtain agreement on the observed cross section for $e^+e^- \rightarrow \text{hadrons}$, the model used above should be modified by the introduction of color.¹¹ The effect of three such colors is to reduce all quark and antiquark distributions by a factor of 3. Then to obtain cross sections we must sum over all colors. The over-all effect is to decrease all

lepton-pair and W production cross sections by a factor of 3.

In principle, the quark distributions in the proton can be determined from lepton-induced reactions. As a check we first compare the presently available $l\bar{l}$ -production data with the predictions of the model. The electromagnetic $l\bar{l}$ -continuum-production cross section in a pp reaction is given by

$$\frac{d\sigma}{dM} = \frac{8\pi\alpha^2}{3M^3} \int_0^1 dx_1 \int_0^1 dx_2 \delta(x_1 x_2 - \tau) x_1 x_2 f(x_1, x_2), \quad (3.5)$$

where

$$\begin{aligned} f(x_1, x_2) = & \frac{4}{9} [u(x_1)\bar{u}(x_2) + u(x_2)\bar{u}(x_1)] \\ & + \frac{1}{9} [d(x_1)\bar{d}(x_2) + d(x_2)\bar{d}(x_1)] \\ & + \frac{1}{9} [\lambda(x_1)\bar{\lambda}(x_2) + \lambda(x_2)\bar{\lambda}(x_1)], \end{aligned} \quad (3.6)$$

and $\lambda, \bar{\lambda}$ are the strange quarks in the proton quark sea. It is well known that the cross section for the production of lepton pairs at large τ is a very sensitive function of the quark and antiquark distributions at large x (i.e., $x \approx 1$). Lepton-induced experiments cannot determine the antiquark distributions accurately enough, especially at large x .

We shall use those distributions obtained by Pakvasa, Parashar, and Tuan.⁶ A distinctive feature of this parametrization is that the antiquark distribution behaves like $(1-x)^{7/2}$ at large x , as proposed originally by Kuti and Weisskopf.⁵ Of all proposed distributions⁵ that we know, this particular choice maximizes the lepton-pair cross sections and gives best agreement with data in the small- s/M^2 region. These distributions are

$$\begin{aligned} u(x) &= u_v(x) + c(x), \\ d(x) &= d_v(x) + c(x), \\ \lambda(x) &= \bar{\lambda}(x) = \bar{u}(x) = \bar{d}(x) \equiv c(x), \\ u_v(x) &= 1.79x^{-1/2}(1-x)^3(1+2.3x), \\ d_v(x) &= 1.107x^{-1/2}(1-x)^{3.1}, \\ c(x) &= 0.1x^{-1}(1-x)^{7/2}. \end{aligned} \quad (3.7)$$

Figures 2, 3, and 4 show the comparison of the model (without color) prediction with the BNL-Columbia experiment,⁸ the MIT-BNL experiment,⁹ and the Fermilab-Columbia-Illinois experiment,¹⁰ respectively. Appropriate longitudinal cutoffs are introduced corresponding to the specific values of each experiment. In Fig. 2 we also plot a curve (dotted) corresponding to a model¹² where the sea-quark distribution is proportional to $(1-x)^9$. Fig-

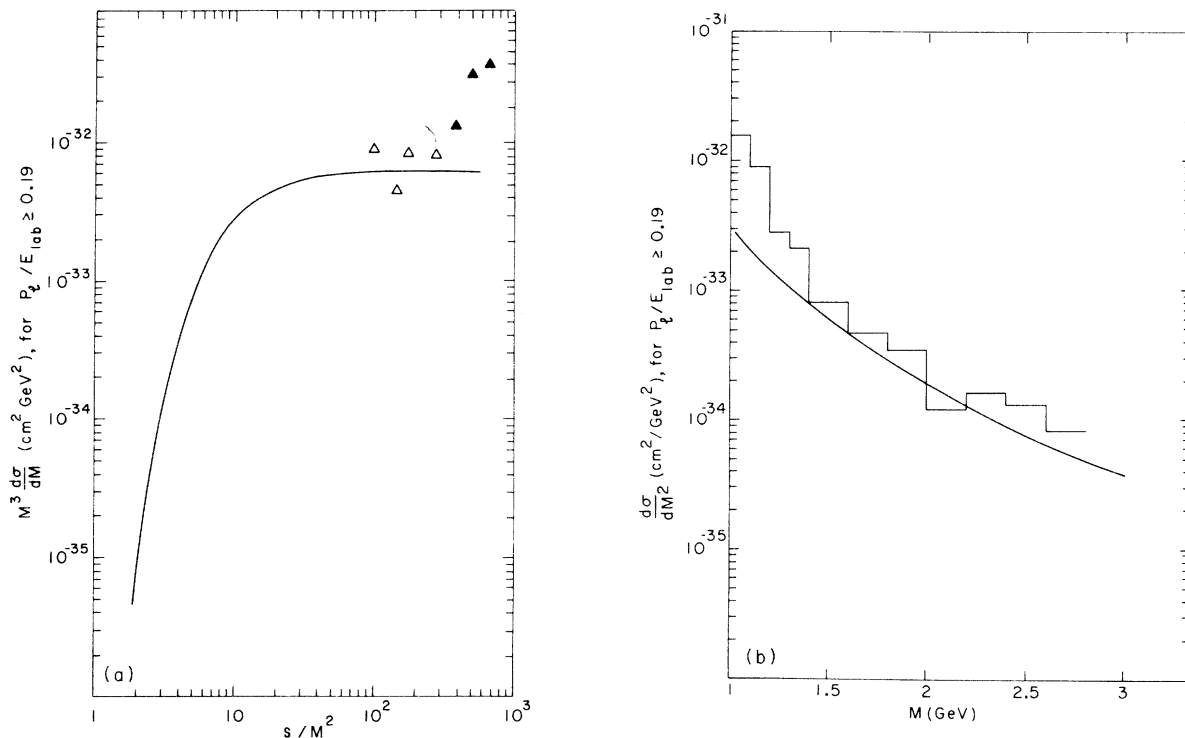


FIG. 4. (a) The dimensionless cross section $M^3 d\sigma/dM$ as a function of s/M^2 . The data points are from Ref. 10 at $E_{\text{lab}} \approx 320$ GeV/c, $1 \text{ GeV} \leq M \leq 2.8$ GeV, and laboratory dilepton $p_{\perp} \approx 60$ GeV/c. Data points for $M \leq 1.5$ GeV are made solid black. The solid curve is the model calculation as discussed in Sec. III. (b) Same calculation and data as in Fig. 4(a) replotted in $d\sigma/dM$ vs. M .

ure 5 summarizes the results of a calculation with dilepton momenta integrated over the entire range; it also shows the “experimental points” integrated over the undetected momentum range according to the model.

Experimental data points for lepton-pair masses less than 1.5 GeV, where the contributions from other sources may dominate, are marked in black. If those black points are ignored, then the agreement between experiment and theory appears remarkable. However, it must be remembered that if color is present then the theoretical curves are lowered by a factor of 3 and a significant discrepancy may exist. We note in any case that a smooth curve can be drawn through the BNL and Fermilab points, which suggests that the data are consistent with scaling.

Using the same quark distributions we can calculate the production cross sections for W^+ shown in Fig. 6. It is noted that the cross section for the production of W^+ is larger than that of W^- , as is evident from the fact that there are more u quarks than d quarks in the proton. In the same figure we also show the corresponding cross sections for $\bar{p}p$ collisions. The cross sections for W^+ and W^- are now equal. The cross sections for

$\bar{p}p$ are about an order of magnitude larger than those for pp interaction. This is a consequence of the fact that there are more antiquarks in the antiproton.

IV. DECAY MODES

An experimental signature for charged- W production would be a peak¹³ in the perpendicular momentum of the produced muon (or electron), assuming the p_{\perp} cutoff of W production to be much smaller than its mass. Figure 7 shows two typical curves indicating the p_{\perp} distributions of the lepton decaying from W 's of 90 GeV and 126 GeV. The smooth curve is the envelope of the peaks of such curves for different masses of W and $s = (400)^2$ GeV² calculated from the parton model.

The hadronic width¹⁴ for W^+ is given by

$$\Gamma(W \rightarrow \text{hadrons}) = \frac{Gm_w^3}{3\pi(2)^{1/2}} R^{l=1}, \quad (4.1)$$

where

$$R^{l=1} = \frac{\sigma(e\bar{e} \rightarrow \text{hadrons})^{l=1}}{\sigma(e\bar{e} \rightarrow \mu\bar{\mu})}. \quad (4.2)$$

The axial-vector contribution was set equal to the

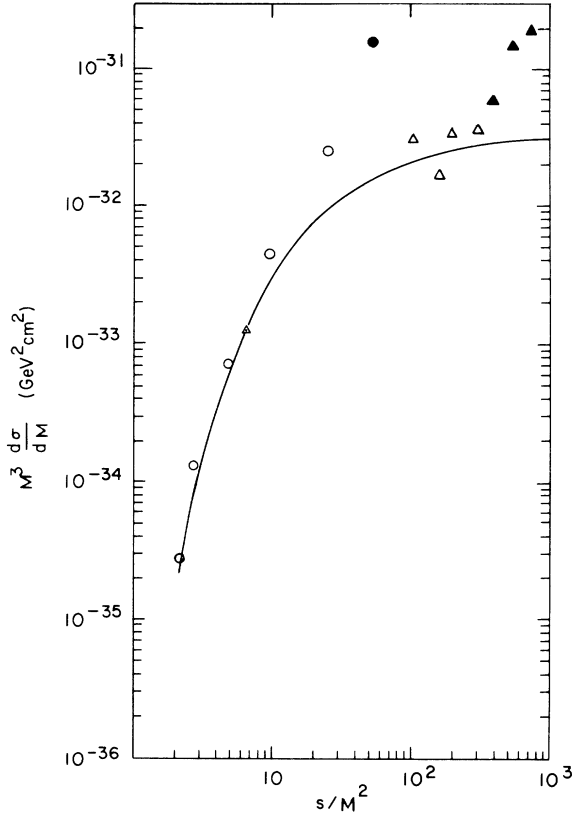


FIG. 5. The dimensionless cross section $M^3 d\sigma/dM$ with the dilepton momentum integrated. Data used are from the same experiments as in Figs. 2, 3, and 4. However, the data points are obtained by integrating over the undetected-momentum range according to the model.

vector contribution. The branching ratio is

$$B = \frac{\Gamma(W \rightarrow \mu\nu) + \Gamma(W \rightarrow e\nu)}{\Gamma(W \rightarrow \text{hadrons})} = \frac{1}{R^{I=1}}. \quad (4.3)$$

To obtain the value of $R^{I=1}$ and B we need specific models. Relying on the fact that the W mass is heavy enough so the asymptotic arguments hold, we estimate $R^{I=1}$ in several quark models. In the simple triplet-quark model, $B=2$; in the color-triplet model, $B=\frac{2}{3}$; in the color-quartet model, $B=\frac{1}{3}$.

Presently¹⁵ $R \approx 5.5$ is measured in e^+e^- collision at c.m. energy $\sqrt{s}=7$ GeV. If the isoscalar component is small and heavy leptons are not produced, then $R^{I=1}=R$. This indicates a sizeable ratio for the experimental observations. But even a logarithmic rise in R , which is suggested by some gauge theories¹⁶ and is not inconsistent with the data,¹⁵ gives $B \approx 0.08$ for $M_W \approx 100$ (GeV/ c^2). Thus the detection through the leptonic modes seems possible.

The signature for W^0 production is a peak in the effective mass of the electron or muon pair. From

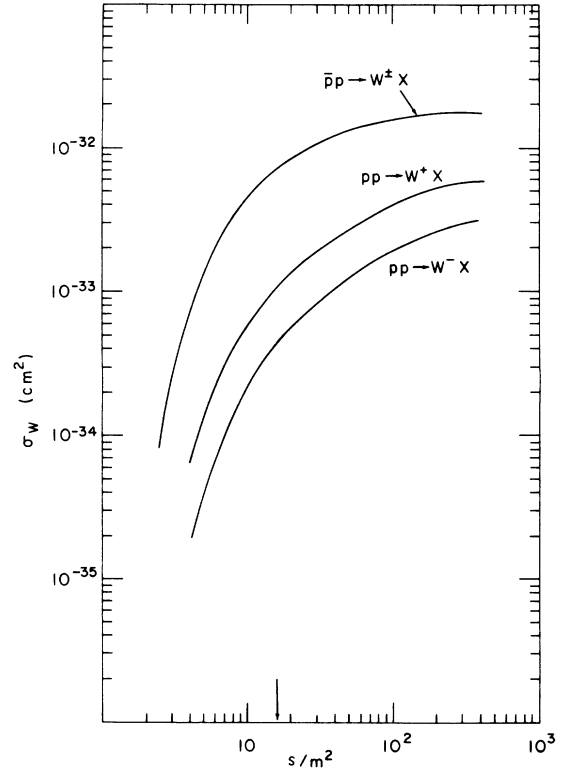


FIG. 6. Production cross section for $pp \rightarrow W^+ X$ and $\bar{p}p \rightarrow W^+ X$, calculated from the model given in Sec. III. The arrow points to the s/M^2 value corresponding to the production of a 100-GeV W meson by a 200-GeV/ c -on-200-GeV/ c storage machine.

Eq. (4.1), the width of such a peak would be of the order of 100 MeV for $m_W \approx 100$ GeV. In contrast, the electromagnetic decay of an ordinary vector meson is expected to be of the order of $\alpha^2 m/3$, which is about a few MeV for a 100 GeV ordinary meson.

V. CONCLUSIONS

The analysis of this article emphasizes the importance of an experimental test of scaling in dilepton production, i.e., the dependence of the cross section $M^3 d\sigma/dM$ on a single variable s/M^2 , where M is the dilepton mass. If scaling is confirmed, then we have a model-independent lower bound for the W -meson production.

We have calculated cross sections for W and lepton-pair production based on a particular Drell-Yan model. Data from experiments at very different energies and over a wide range of s/M^2 (neglecting data points with $M < 1.5$ GeV) show remarkable agreement with the model for the case without color. For the case with color, the model prediction is systematically lower than all experimental points. In any case, the fact that the data lie on a smooth curve does suggest

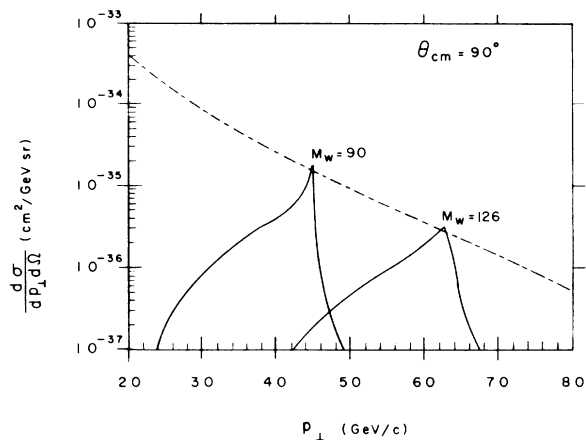


FIG. 7. The double-differential cross section of the lepton at $\theta_{c.m.} = 90^\circ$ from a produced W meson on pp reaction at $s = (400)^2 \text{ GeV}^2$ for two different W masses.

scaling. On this basis, W 's would be copiously produced in a 200 GeV on 200 GeV intersecting storage ring.³

We have also calculated the leptonic-branching ratios of W decay based upon various quark models. They are typically of order 10% and thus the observation of W 's through their leptonic decays should be possible.

ACKNOWLEDGMENTS

The paper is an outcome of the summer study of ISABELLE, 1975. We have benefitted greatly from many members of the summer study, especially Dr. L. M. Lederman, Dr. C. Rubbia, Dr. R. F. Peierls, Dr. S. B. Treiman, and Dr. T. L. Trueman. We would like to thank Dr. M. Chen, Dr. W. Lee, Dr. T. A. O'Halloran, and Dr. S. C. C. Ting for discussions on their data.

*Work supported by the Energy Research and Development Administration.

¹S. Weinberg, in proceedings of the Second International Conference on Elementary Particles, Aix-en-Provence, 1973 [J. Phys. (Paris) Suppl. **34**, C1-45 (1973)].

²J. G. Morfin, in *Proceedings of the 1975 International Symposium on Lepton and Photon Interactions at High Energies, Stanford, California*, edited by W. T. Kirk (SLAC, Stanford, 1976).

³Proposal for construction of a proton-proton storage accelerator facility, BNL Report No. BNL 20161 (1975).

⁴Y. Yamaguchi, *Nuovo Cimento* **43**, 193 (1966); L. M. Lederman and B. G. Pope, *Phys. Rev. Lett.* **27**, 765 (1971); L. M. Lederman and D. H. Saxon, *Nucl. Phys.* **B63**, 315 (1973).

⁵The literature on the Drell-Yan model as it applies to this process is rather extensive. We mention some of the early papers here and refer to the recent articles at places where they are relevant; S. D. Drell and T.-M. Yan, *Phys. Rev. Lett.* **25**, 316 (1970); *Ann. Phys.* (N.Y.) **66**, 578 (1971); J. Kuti and V. Weisskopf, *Phys. Rev. D* **4**, 3418 (1971); P. V. Landshoff and J. C. Polkinghorne, *Nucl. Phys.* **B33**, 221 (1971); *ibid.* **B36**, 643 (1972); S. M. Berman, J. D. Bjorken, and J. B. Kogut, *Phys. Rev. D* **4**, 3388 (1971); Yu. A. Golubkov, A. A. Ivanilov, Yu. P. Nikitin, and G. V. Rozhnov, *Yad. Fiz.* **18**, 393 (1973) [*Sov. J. Nucl. Phys.* **18**, 203 (1974)]; G. Altarelli *et al.*, *Nucl. Phys.* **B92**, 413 (1975).

⁶J. Pakvasa, D. Parashar, and S. F. Tuan, *Phys. Rev. D* **10**, 2124 (1974); **11**, 214 (1975). When we were finishing our manuscript we were informed by Dr. S. F. Tuan and L. Pilachowski that Z_1 in this reference should be 1.74, not 1.79. This means that the coefficient for $u_\nu(x)$ in Eq. (3.7) should be 1.74, not 1.79. This change reduces our theoretical curves in all figures by a small insignificant amount.

⁷S. Weinberg, *Phys. Rev. Lett.* **19**, 1264 (1967); A. Salam, in *Elementary Particle Physics: Relativis-*

tic Groups and Analyticity (Nobel Symposium No. 8), edited by N. Svartholm (Almqvist, Stockholm, 1968), p. 367.

⁸J. H. Christenson *et al.*, *Phys. Rev. Lett.* **25**, 1523 (1970). To obtain the pp cross section from their p -uranium data, the authors divided a factor of $A^{2/3}$ from the pU cross section, though a factor of A is more appropriate. Clearly here there is an over-all normalization problem. L. M. Lederman, Columbia report, 1974 (unpublished). The J and ψ' productions are subtracted.

⁹J. J. Aubert *et al.*, *Phys. Rev. Lett.* **33**, 1404 (1974); S. C. C. Ting, in *Proceedings of the 1975 International Symposium on Lepton and Photon Interactions at High Energies, Stanford, California*, edited by W. T. Kirk (SLAC, Stanford, 1976).

¹⁰T. O'Halloran, in *Proceedings of the 1975 International Symposium on Lepton and Photon Interactions at High Energies, Stanford, California*, edited by W. T. Kirk (SLAC, Stanford, 1976).

¹¹O. W. Greenberg, *Phys. Rev. Lett.* **13**, 598 (1964); M. Gell-Mann, *Acta Phys. Austriaca* **9**, 733 (1972); W. A. Bardeen, H. Fritzsch, and M. Gell-Mann, in *Scale and Conformal Symmetry in Hadron Physics*, edited by R. Gatto (Wiley, New York, 1973), p. 139; M. Gell-Mann, in *Proceedings of the XVI International Conference on High Energy Physics, Chicago-Batavia, Ill., 1972*, edited by J. D. Jackson and A. Roberts (NAL, Batavia, Ill., 1973), Vol. V, p. 333.

¹²H. P. Paar and E. A. Paschos, *Phys. Rev. D* **10**, 1502 (1974). For still another parametric form see G. Farrar, *Nucl. Phys.* **B77**, 429 (1974); V. Barger and R. J. N. Phillips, *ibid.* **B73**, 269 (1974).

¹³R. L. Jaffe and J. R. Primack, *Nucl. Phys.* **B61**, 317 (1973). This article contains numerous gauge-model estimates, which complement the present article.

¹⁴J. D. Bjorken, *Phys. Rev.* **148**, 1467 (1966); V. N. Gribov, B. L. Ioffe, and I. Ya. Pomeranchuk, *Phys. Lett.* **24B**, 554 (1967); L.-F. Li and E. A. Paschos,

Phys. Rev. D 3, 1178 (1971).
¹⁵R. Schwitters and F. Gilman, in *Proceedings of the 1975 International Symposium on Lepton and Photon Interactions at High Energies, Stanford, California,*

edited by W. T. Kirk (SLAC, Stanford, 1976).
¹⁶T. Appelquist and H. Georgi, Phys. Rev. D 8, 4000 (1973); A. Zee, *ibid.* 8, 4038 (1973).